Journal of Colloid and Interface Science 360 (2011) 233–238

Contents lists available at ScienceDirect

Journal of Colloid and Interface Science

www.elsevier.com/locate/jcis

Effect of surface acidity and basicity of aluminas on asphaltene adsorption and oxidation

Nashaat N. Nassar *, Azfar Hassan, Pedro Pereira-Almao *

Department of Chemical & Petroleum Engineering, Alberta Ingenuity Centre for In-Situ Energy, University of Calgary, Calgary, Alberta, Canada

ARTICLE INFO

Article history:
Received 23 February 2011
Accepted 17 April 2011
Available online 27 April 2011

Keywords:
Asphaltenes
Oxidation
Adsorption
Activation energy
Alumina

ABSTRACT

This study investigates the effect of surface acidity and basicity of aluminas on asphaltene adsorption followed by air oxidation. Equilibrium batch adsorption experiments were conducted at 25 °C with solutions of asphaltenes in toluene at concentrations ranging from 100 to 3000 g/L using three conventional alumina adsorbents with different surface acidity. Data were found to better fit to the Freundlich isotherm model showing a multilayer adsorption. Results showed that asphaltene adsorption is strongly affected by the surface acidity, and the adsorption capacities of asphaltenes onto the three aluminas followed the order acidic > basic and neutral. Asphaltenes adsorbed over aluminas were subjected to oxidation in air up to 600 °C in a thermogravimetric analyzer to study the catalytic effect of aluminas with different surface acidity. A correlation was found between Freundlich affinity constant ($1/n$) and the catalytic activity. Basic alumina that has the lowest $1/n$ value, depicting strongest interactions, has the highest catalytic activity, followed by neutral and acidic aluminas, respectively.

1. Introduction

Heavy polar hydrocarbons, such as asphaltenes, are the main hindrances in production and processing of heavy oils due to their complexity and unidentifiable chemical structure [1–5]. They usually are defined as the fraction of heavy oil that is insoluble in low molecular weight paraffin such as *n*-heptane while soluble in light aromatic hydrocarbons such as toluene [6]. Asphaltene structure consists of many series of relatively large molecules containing aromatic rings, relatively short paraffinic branches, and several heteroaromatic and napthenic rings containing one or several heteroatoms such as nitrogen, oxygen, sulfur, and metals such as vanadium, iron, and nickel. Furthermore, asphaltenes are surface active that stabilize undesirable emulsions of water-in-oil and create oil–water separation difficulties [7,8]. Asphaltenes create a number of problems for crude oil production, processing and transportation, such as reservoir damage, well-bore plugging, pipeline and tank clogging, and catalyst deactivation and poisoning [9,10]. As a result, asphaltenes make heavy oil upgrading challenging and costly as well as environmentally unfriendly. Currently, oil industry is mostly focusing on cracking and hydrogenating of asphaltenes along with other heavy molecules to produce lighter fractions [11,12]. Others are focusing on separating asphaltenes for gasification or combustions [13–16]. Several studies have been reported on the adsorption of asphaltenes onto solid surfaces [14,17–23]. Adsorption process is generally studied by extracting asphaltenes from the heavy oil and resolubilizing them in a model solvent, such as toluene or heptol (heptane + toluene). Based on these studies, two different types of adsorption isotherms have been reported. Langmuir-type isotherms indicating that asphaltene molecules form monolayer coverage on the solid surface were observed in most solid surfaces [5,24–26]. Multilayer adsorption isotherms have been reported as well [4,24,27–29]. Multilayer behavior was attributed to the aggregate formation and precipitation of asphaltenes in the bulk due to asphaltene association and further formation of hemimicelles. It is noteworthy that the adsorption of asphaltene onto solid surfaces occurs due to favorable interactions of the asphaltene species with the solid surface. A number of interparticle forces are responsible for this successful interaction, individually or collectively, between asphaltenes and the surface resulting from functionalized groups on the asphaltenes, including carboxylic, pyrrolic, pyridininc, thiophenic, and sulfite groups [30]. The major forces that could contribute to these interactions are van der Waals, electrostatic, charge transfer, hydrogen bonding, and steric interactions [2,31]. Despite the extensive studies on the asphaltene adsorption onto solid surfaces, to the best of our knowledge, no single work has been reported on the effect of solid surface acidity and basicity on the asphaltene adsorption behavior. Furthermore, little attention has been given to the effect of solid surface catalytic activity toward asphaltene oxidation. In this study, three types of aluminas having similar textural properties but differing in surface acidity are employed for asphaltene adsorption followed by complete oxidation in order to

* Corresponding authors.
E-mail addresses: nassar@ucalgary.ca (N.N. Nassar), ppereira@ucalgary.ca (P. Pereira-Almao).

0021-9797/$ - see front matter © 2011 Elsevier Inc. All rights reserved.
doi:10.1016/j.jcis.2011.04.056

study the effect of surface acidity or basicity on the adsorption and oxidation processes. To the best of our knowledge, a work relating asphaltene adsorption to surface acidity or basicity and its catalytic effect toward oxidation is conducted for the first time. Alumina is commonly used as a support for designing catalysts suitable for heavy oil upgrading [10,32]. This study will provide more insight into the influence of surface acidity or basicity of the support toward asphaltene adsorption and oxidation.

2. Materials and methods

2.1. Alumina adsorbents

Three types of aluminas of different surface acidity were obtained from Sorbent Technologies, Inc., Atlanta, GA, namely alumina acid (AA) with pH 4.5, alumina neutral (AN) with pH 7.5, and alumina basic (AB) with pH 10. All aluminas have particle size between 50 and 200 μm. Its proposed structures are shown in Fig. 1. Acidic alumina was prepared by giving an acid wash to alumina surface. Similarly, basic alumina was made by washing the alumina surface with a base. Details of preparation procedure are kept confidential by the vendor.

2.2. Nitrogen physisorption

Textural properties of the aluminas were obtained by using Micromeritics Tristar II 3020 instrument. About 100 mg of the sample was pretreated overnight at 150 °C. Nitrogen physisorption experiments were carried out at 77 K. The equilibration time for N_2 physisorption during analysis was 10 s. Surface areas were calculated using Brunauer–Emmet–Teller (BET) equation. Table 1 lists the specifications and textural properties of different surface aluminas used in this study.

2.3. Adsorbate

Asphaltenes were used as adsorbate in this study. The asphaltenes were prepared from Athabasca bitumen sample in Alberta.

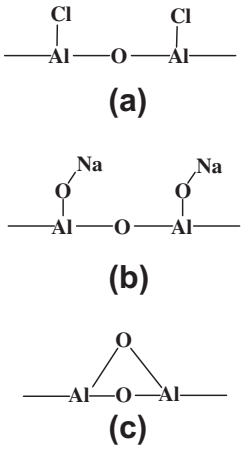

Fig. 1. Proposed chemical structure of (a) acidic, (b) basic, and (c) neutral aluminas.

Table 1
Textural properties of selected aluminas with varying acidity.

Type of alumina	BET surface area (m^2/g)	Pore volume (cm^3/g)	Avg. pore size (A)
Acidic (AA)	128	0.2738	60
Basic (AB)	156	0.2909	54
Neutral (AN)	154	0.2751	52

Solvents used in the precipitation and extraction of asphaltenes were *n*-heptane (99% HPLC grade, Sigma Aldrich, ON) and toluene (analytical grade, EMD, MERCK, NJ).

2.4. Heavy oil model solutions

Asphaltenes were extracted from bitumen sample with addition of *n*-heptane following the technique described in previous studies [33]. Briefly, a specified amount of bitumen was mixed with *n*-heptane at a ratio of 1:40 (g/mL). The solution was then sonicated in a water bath at 25 °C for 2 h and left shaking at 300 rpm for 1 day to equilibrate. Black precipitated asphaltenes settled at the bottom and then were collected after decanting the supernatant. Then, the precipitated asphaltenes were washed with fresh *n*-heptane at a ratio of 1:4 (g/mL), centrifuged at 5000 rpm for 5 min and left to stand overnight. The asphaltenes were separated from the final solution by filtration using an 8-μm Whatman filter paper. The cake was washed with *n*-heptane several times until the color of the asphaltenes became shiny black. The resultant asphaltenes were homogenized and fined using pestle and mortar and left to dry at room temperature in a hood until no change in mass was observed. The model heavy oil solutions for the batch adsorption experiments were prepared by dissolving a specified amount of the asphaltenes in toluene. The initial concentration of asphaltene solutions used in the adsorption experiments ranged from 10 to 3000 mg/L.

2.5. Adsorption experiments

Batch adsorption experiments were carried out in 20-ml vials by mixing together a 100 mg adsorbent with a 10 ml of the prepared heavy oil solutions at 25 °C. The contents in the vials were agitated at 200 rpm by placing them in a temperature incubator and allowed to equilibrate for 24 h, as it was an adequate time to achieve equilibrium. The alumina containing adsorbed asphaltenes was separated from the mixture by centrifugation at 5000 rpm for 30 min. Then the aluminas were placed in vacuum oven for 24 h to evaporate any remaining toluene. After that, the aluminas were analyzed for its asphaltenes content using a thermogravimetric analysis/differential scanning calorimetry (TGA/DSC) analyzer (SDTQ600, TA Instruments, Inc., New Castle, DE).

2.6. Oxidation and thermal analysis of asphaltenes

Thermal analysis of asphaltenes before and after adsorption over alumina was carried out using a thermogravimetric analyzer. About 5–10 mg of sample was heated under hydrocarbon-free ultra high purity (UHP) grade air atmosphere. The air flow rate was kept at 100 cm^3/min. Fresh alumina without asphaltenes was heated to 1000 °C at a heating rate of 10 °C/min to get a complete profile of mass loss and heat changes. For adsorption isotherms, virgin asphaltenes and asphaltenes adsorbed onto different aluminas were heated up to 900 °C in air at a heating rate of 10 °C/min. For oxidation kinetic studies, mass loss and heat changes up to 600 °C were recorded in separate experiments and used in calculations.

3. Results and discussion

3.1. Equilibrium isotherms of asphaltenes adsorption onto alumina surfaces

The adsorption of asphaltenes onto alumina surface depends on the type and strength of interactions between the asphaltenes and the surface. This interaction depends on the functional groups present on the surface as well as the part of asphaltenes in the

vicinity of surface approaching for bonding. Molecular interactions during adsorption result from intermolecular forces. These intermolecular forces are typically divided into three basic categories: dispersion forces, polar forces, and ionic forces. All interactions between molecules and surface are composites of these three forces.

Dispersion attractive forces are typically those that occur between hydrocarbons and nonpolar molecules and are weak in nature. Polar interactions, on the other hand, arise from electrical forces between localized charges resulting from permanent or induced dipoles. Polar interactions can be very strong and result in molecular associations like a weak chemical bond. Hydrogen bonding is one typical example of polar interaction. Fig. 1 shows the surface groups present on acidic, basic, and neutral aluminas, which imply that different counter ions exist on the surface. Fig. 2 shows some of the molecular fragments found by Strausz et al. [34] in Athabasca asphaltenes. In order to examine the level of involvement of surface acidity or basicity of aluminas in bonding to the asphaltenes, adsorption of asphaltenes onto various surfaces of alumina was tested for sufficiently long times (24 h). Asphaltene equilibrium concentration in the supernatant and the adsorbed amount of asphaltenes onto different aluminas were calculated and presented in Fig. 3. It was found that all the three aluminas, considered in this study, showed affinity toward asphaltene adsorption. This can be attributed to the high surface areas of aluminas as well as to the interaction of asphaltenes with the counter ions present on alumina surface. The effect of different functional groups present on the surfaces of aluminas is evident from the fact that acidic alumina (AA) has the lowest surface area

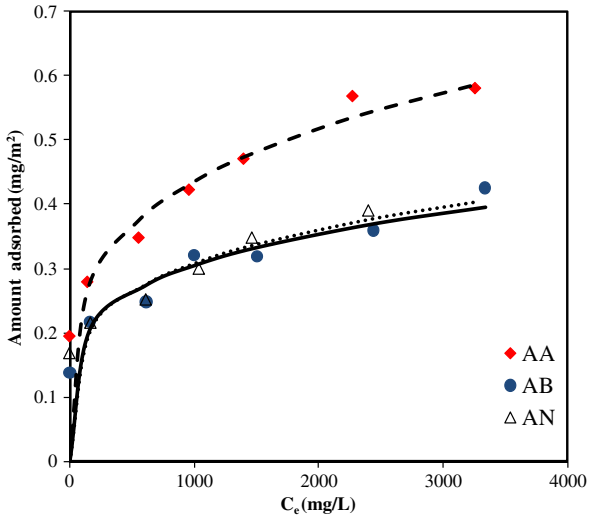

Fig. 3. Adsorption isotherms of asphaltenes onto different alumina adsorbents. Adsorbent dose, 10 g/L; shaking rate, 200 rpm; contact time, 24 h; and temperature, 25 °C. Points are experimental data, and the solid lines are from Freundlich model (Eq. (2)).

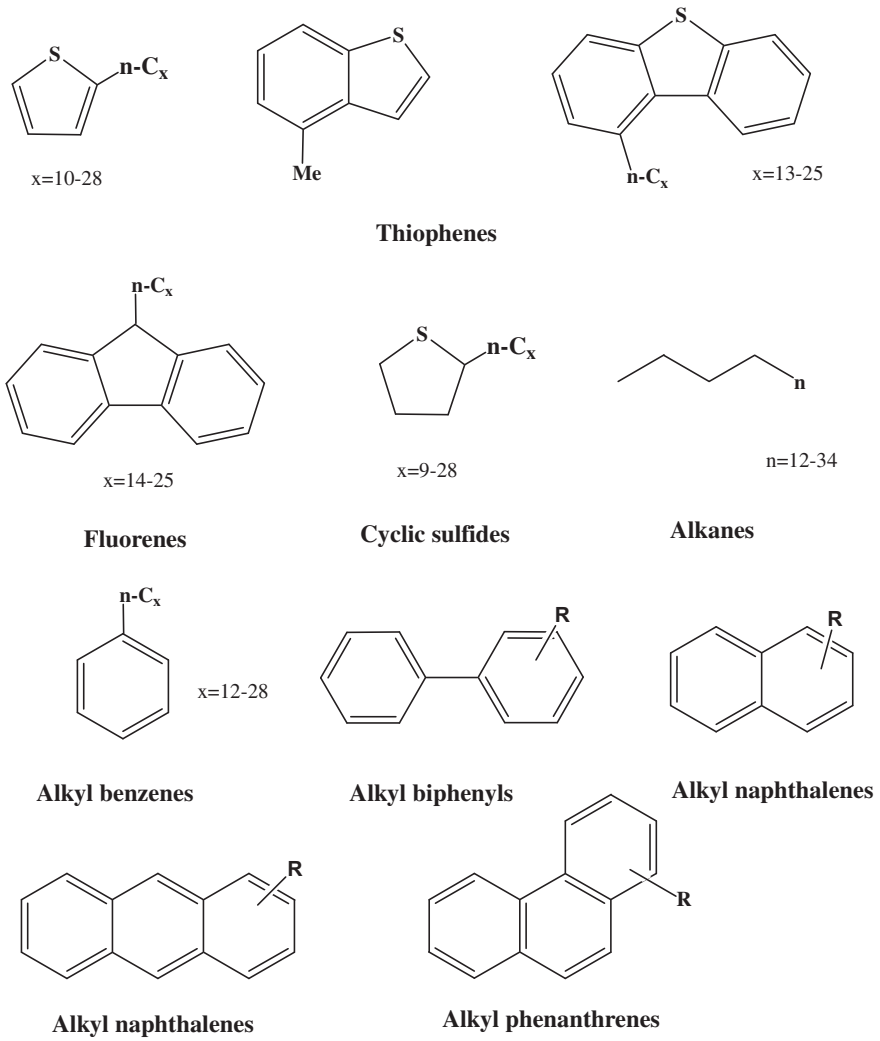

Fig. 2. Asphaltene structure fragments [34].

than basic (AB) and neutral (AN) aluminas, but has the highest adsorption. It appears that acidic surface facilitates asphaltene adsorption.

3.2. Isotherm models

To further investigate the adsorption behavior, adsorption isotherms were studied at 25 °C. Both Langmuir and Freundlich models were tested to find the most suitable isotherm model. Langmuir and Freundlich models are defined as Eqs. (1) and (2), respectively. The linear form of the Langmuir and Freundlich models are shown as Eqs. (3) and (4), respectively.

$$Q_e = \frac{Q_{\max} K_L C_e}{1 + K_L C_e} \tag{1}$$

$$Q_e = K_F C_e^{1/n} \tag{2}$$

$$\frac{C_e}{Q_e} = \frac{1}{Q_{\max} K_L} + \frac{C_e}{Q_{\max}} \tag{3}$$

$$\mathrm{Log}(Q_e) = \mathrm{Log}(K_F) + \frac{1}{n}\mathrm{Log}(C_e) \tag{4}$$

where Q_e is the amount of asphaltene adsorbed onto the adsorbent (mg/m^2), C_e is the equilibrium concentration of asphaltenes in supernatant (mg/L), K_L is the Langmuir equilibrium adsorption constant related to the affinity of binding sites (L/mg), and Q_{max} is the maximum adsorption capacity for complete monolayer coverage (mg/m^2). K_F and $1/n$ are Freundlich constants. K_F is roughly an indicator of the adsorption capacity ($(mg/m^2)(L/mg)^{1/n}$), and $1/n$ is the adsorption intensity factor (unitless). Specifically, a larger K_F value suggests a greater adsorption capacity, and a lower $1/n$ value indicates stronger adsorption strength.

Linearity obtained in case of both models (Figs. 4 and 5) confirms their applicability in the adsorption of asphaltenes over different alumina surfaces. The adsorption data were fitted very well for both Freundlich and Langmuir models. Nonetheless, chi-square test (χ^2) was used to measure the goodness-of-fit as per Eq. (5) [35].

$$\chi^2 = \sum \frac{(Q_e - Q_{e\mathrm{Model}})^2}{Q_{e\mathrm{Model}}} \tag{5}$$

where Q_e and $Q_{e_{\mathrm{Model}}}$ are the equilibrium adsorbed amount of asphaltenes obtained experimentally and by modeling, respectively.

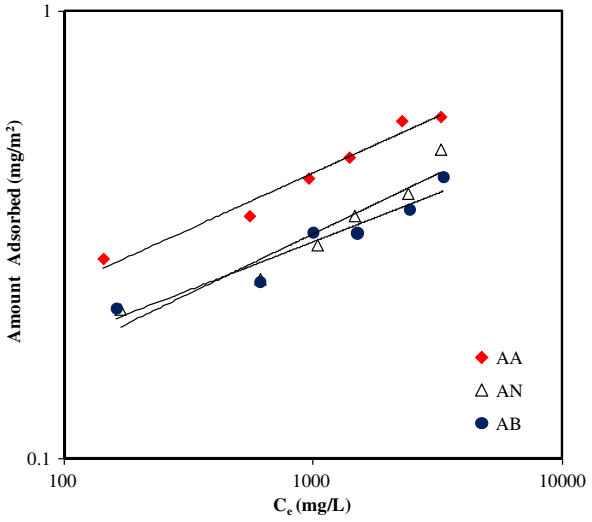

Fig. 4. Freundlich isotherms of asphaltenes onto different aluminas. Adsorbent dose, 10 g/L; shaking rate, 200 rpm; contact time, 24 h; and temperature, 25 °C.

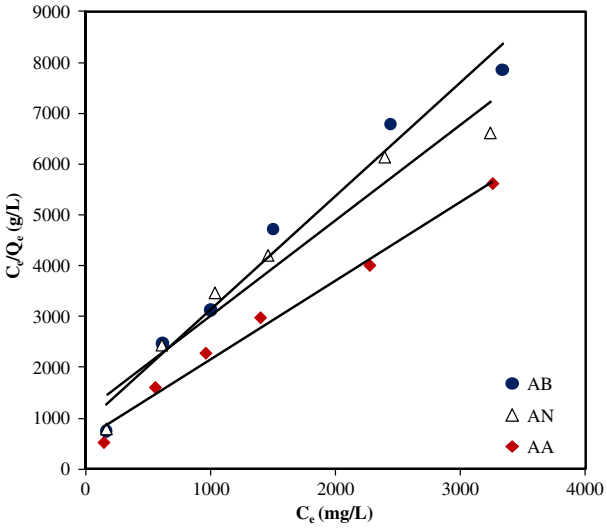

Fig. 5. Langmuir isotherms of asphaltenes onto different aluminas. Adsorbent dose, 10 g/L; shaking rate, 200 rpm; contact time, 24 h; and temperature, 25 °C.

The smaller χ^2 value indicates the better agreement with the model. The adsorption constants obtained from the isotherms together with χ^2 values are listed in Table 2. Clearly, Freundlich model seems to be the best-fitting model for the experimental data. It is noteworthy that Langmuir model assumes that adsorption occurs on a homogeneous surface, while Freundlich model describes adsorption where the adsorbent has a heterogeneous surface with adsorption sites that have different adsorption energies. The values of $(1/n)$ in Table 2 indicate that n values are greater than unity suggesting that asphaltenes are favorably adsorbed by the different alumina surfaces. Clearly, acidic alumina has the highest adsorption capacity; however, the adsorption affinity is lower than basic and neutral aluminas. Again, this supports that surface acidity/basicity plays role in the adsorption process.

3.3. Oxidation of adsorbed asphaltenes over aluminas

To further investigate the effect of surface acidity/basicity, the catalytic effect of the three types of aluminas containing adsorbed asphaltenes was tested by performing asphaltene oxidation. Thermogravimetric analysis was conducted to determine the weight loss when heated in air, with linear increase in temperature. Reactivity of virgin asphaltenes toward oxidation before adsorption was also tested for comparison. The mass of sample was kept to a minimum to avoid mass transfer limitations. Percentage conversion ratio (α) was determined from the weight loss data as per the following equation:

$$\alpha = \frac{w_o - w_t}{w_o - w_\infty} \tag{6}$$

where w_o is the initial sample mass, w_o is the final sample mass, and w_t is the sample mass at any time. Fig. 6 shows a plot of percentage conversion ratio (α) of asphaltenes in the absence and presence of different aluminas, as a function of temperature. It appears that thermal decomposition of virgin asphaltenes started beyond 350 °C and reached a maximum rate at around 475 °C, showing occurrence of combustion reaction during oxidation. It is evident from the figure that adsorption of asphaltene over aluminas greatly enhanced the oxidation process, depicting catalytic effect of the support. Oxidation process involving thermal cracking started as early as 40 °C. This decrease in temperature for oxidation reaction clearly shows the catalytic behavior of aluminas toward oxidation of asphaltenes.

Table 2
Langmuir and Freundlich constants for asphaltene adsorption onto different aluminas at 25 °C.

Adsorbent	Freundlich constants				Langmuir constants			
	K_F (mg/m^2)(L/mg)$^{1/n}$	$1/n$ (unitless)	R^2	χ^2	K_L (L/mg)	Q_m (mg/m^2)	R^2	χ^2
AA	0.0763	0.2519	0.97	0.005	0.0026	0.65	0.99	0.073
AB	0.0685	0.2162	0.93	0.007	0.0025	0.45	0.97	0.071
AN	0.0602	0.2372	0.95	0.005	0.0015	0.50	0.95	0.123

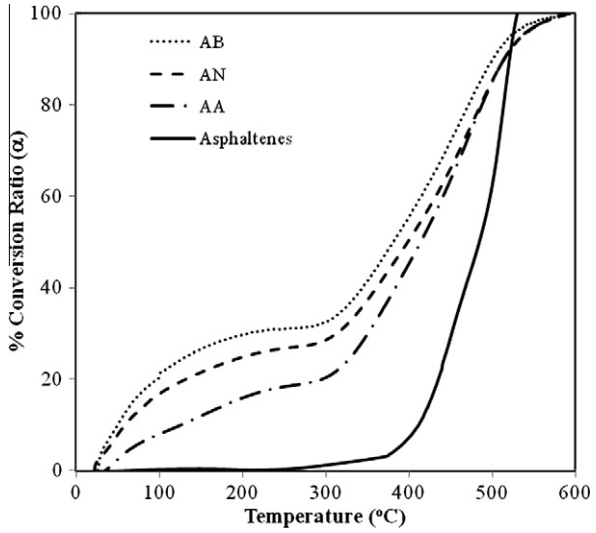

Fig. 6. Percentage conversion ratio curves of asphaltene oxidation in the presence and absence of different aluminas.

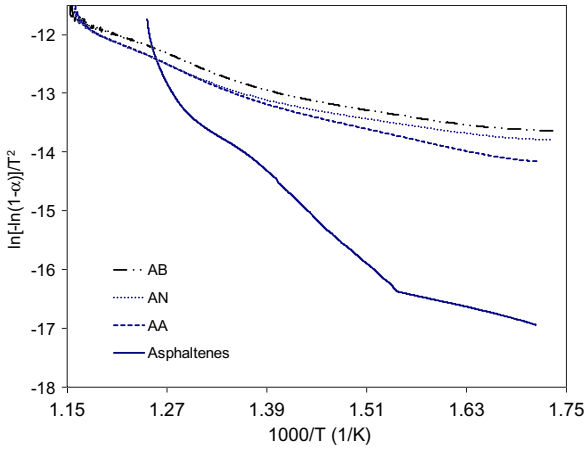

Fig. 7. Oxidation of asphaltenes in the presence and absence of different types of aluminas.

3.4. Estimation of activation energies

Activation energies required for the oxidation reactions of asphaltenes in the presence and absence of alumina were calculated by using thermal analysis data following the method developed by Coats and Redfern [36]. Coats–Redfern method is an integral method of processing the TGA data, which deals with only one weight loss curve to get activation energy. The process is as follows:

According to Arrhenius equation, the conversion rate can be expressed by:

$$\frac{d\alpha}{dt} = Ae^{-E_a/RT} f(\alpha) \tag{7}$$

where A is the pre-exponential factor ($1/s$), E_a is the activation energy (kJ/mol), R is the ideal gas constant (8.314 J/mol K), T is the reaction temperature in Kelvin, and $f(\alpha)$ is the reaction mechanism function. Assuming $f(\alpha) = (1-\alpha)^n$, where n is the order of the reaction, then integration of Eq. (7) yields:

$$\frac{AR}{\beta E_a}\left(1-\frac{2RT}{E_a}\right)\exp\frac{-E_a}{RT} = \begin{cases} \ln\left(\frac{-\ln(1-\alpha)}{T^2}\right), & n=1 \\ \ln\left(\frac{1-(1-\alpha)^n}{(1-\alpha)T^2}\right), & n>1 \end{cases} \tag{8}$$

where $\beta = \frac{dT}{dt}$. If n is known, then a plot of the right hand side of Eq. (8) versus $\frac{1}{T}$ gives a straight line with a slope $= \frac{E_a}{R}$ [36]. Some deviation from straight line may occur due to the presence of competitive reactions or change in reaction mechanism with increase in temperature, which results in different activation energies [15,37–39]. Fig. 7 shows the plot of $\ln\left(\frac{\ln(1-\alpha)}{T^2}\right)$ versus $\frac{1}{T}$. By employing Coats–Redfern method, the values of activation energy were estimated for the oxidation of asphaltenes in the presence and absence of nanoparticles. The values determined are listed in Table 3. For virgin asphaltenes, the activation energy was calculated for three distinct temperature regions between 227 and 514 °C. As shown in Table 3, the activation energy of asphaltenes decreased significantly in the presence of aluminas in the following order AB > AN > AA.

Table 3
Calculated activation energies for asphaltenes in the presence and absence of aluminas at different temperatures.

		(227–372 °C)	(372–467 °C)	(467–514 °C)
Virgin asphaltenes				
	E_a (kJ/mol)	42	108	91
	R^2	0.982	0.999	0.98
Asphaltenes adsorbed onto alumina		(320–355 °C)	(>355 °C)	
AA	E_a (kJ/mol)	27.2	52.0	–
	R^2	0.997	0.999	
AN	E_a (kJ/mol)	17.9	47.0	–
	R^2	0.995	0.995	
AB	E_a (kJ/mol)	18.8	44.7	–
	R^2	0.992	0.997	

3.5. Relationship between adsorption affinity and catalytic activity of aluminas

It was interesting to note that the surface basicity of alumina affects the catalytic activity; the higher the surface basicity, the better was the catalytic activity. It is noteworthy seeing that the Freundlich affinity factor ($1/n$), which is an indicator of adsorbate–adsorbent interaction correlates with the catalytic activity (represented by % conversion) as presented in Fig. 8. It appears that the catalytic activity increases as ($1/n$) values decreases. Clearly, basic alumina that has the lowest $1/n$ value depicting strongest interactions also has the lowest value of E_a, consequently showing highest catalytic activity.

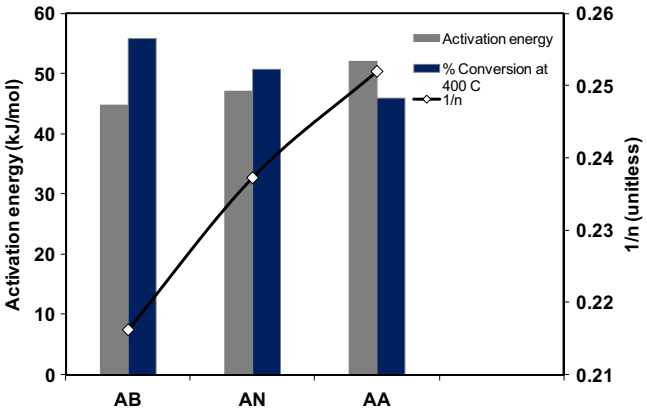

Fig. 8. Relationship between adsorption affinity ($1/n$) and catalytic activity of different aluminas varying surface acidity.

4. Conclusions

In this study, three types of aluminas with different surface acidity have been investigated for adsorption and oxidation of asphaltenes. All three aluminas with varying acidity adsorb asphaltenes efficiently. Freundlich adsorption model gives a good fitting for the adsorption isotherms, suggesting a multilayer adsorption. It was found that adsorption capacity is proportional to surface acidity of aluminas. Acidic alumina has the highest adsorption. On the other hand, basic alumina has the highest catalytic activity toward asphaltene oxidation. Interestingly, a correlation was found to exist between Freundlich affinity constant ($1/n$) and the catalytic activity. Further increase in adsorption affinity, i.e. decrease in $1/n$ values, favors the catalytic activity of the adsorbent. To the best of our knowledge, this is the first time that a correlation between adsorption affinity and catalytic activity has been demonstrated.

Acknowledgment

The authors acknowledge the financial support provided by Carbon Management Canada Inc. (CMC).

References

[1] H. Toulhoat, C. Prayer, G. Rouquet, Colloids Surf., A 91 (C) (1994) 267.
[2] O.P. Strausz, P. Peng, J. Murgich, Energy Fuels 16 (4) (2002) 809.
[3] W.A. Abdallah, S.D. Taylor, Nucl. Instrum. Methods Phys. Res., Sect. B 258 (1) (2007) 213.
[4] A.W. Marczewski, M. Szymula, Colloids Surf., A 208 (1–3) (2002) 259.
[5] B.J. Marlow, G.C. Sresty, R.D. Hughes, O.P. Mahajan, Colloids Surf. 24 (4) (1987) 283.
[6] Y. Bouhadda, D. Bormann, E. Sheu, D. Bendedouch, A. Krallafa, M. Daaou, Fuel 86 (12–13) (2007) 1855.
[7] J.D. McLean, P.K. Kilpatrick, J. Colloid Interface Sci. 196 (1) (1997) 23.
[8] J.D. McLean, P.K. Kilpatrick, J. Colloid Interface Sci. 189 (2) (1997) 242.
[9] I. Mochida, Z. Xing Zhe, K. Sakanishi, Fuel 67 (8) (1988) 1101.
[10] F. Melo Faus, P. Grange, B. Delmon, Appl. Catal. 11 (2) (1984) 281.
[11] P. Danial-Fortain, T. Gauthier, I. Merdrignac, H. Budzinski, Catal. Today 150 (3–4) (2010) 255.
[12] T. Gauthier, P. Danial-Fortain, I. Merdrignac, I. Guibard, A.-A. Quoineaud, Catal. Today 130 (2–4) (2008) 429.
[13] S. Saraji, L. Goual, M. Piri, Energy Fuels 24 (11) (2010) 6009.
[14] F. López-Linares, L. Carbognani, C. Sosa-Stull, P. Pereira-Almao, R.J. Spencer, Energy Fuels 23 (4) (2009) 1901.
[15] N.N. Nassar, A. Hassan, P. Pereira-Almao, Energy Fuels 25 (2011) 1017.
[16] C. Sosa-Stull, Presented at the 235th ACS National Meeting, New Orleans, LA, United States, 2008.
[17] L. Carbognani, M.F. González, F. Lopez-Linares, C. Sosa Stull, P. Pereira-Almao, Energy Fuels 22 (3) (2008) 1739.
[18] M.F. González, C.S. Stull, F. López-Linares, P. Pereira-Almao, Energy Fuels 21 (1) (2006) 234.
[19] F. López-Linares, L. Carbognani, M.F. González, C. Sosa-Stull, M. Figueras, P. Pereira-Almao, Energy Fuels 20 (6) (2006) 2748.
[20] S. Acevedo, M.A. Ranaudo, G. Escobar, L. Gutiérrez, P. Ortega, Fuel 74 (4) (1995) 595.
[21] K. Sakanishi, I. Saito, I. Watanabe, I. Mochida, Fuel 83 (14–15) (2004) 1889.
[22] M.S. Akhlaq, P. Götze, D. Kessel, W. Dornow, Colloids Surf., A 126 (1) (1997) 25.
[23] J. Castillo, S. Goncalves, A. Fernández, V. Mujica, Opt. Commun. 145 (1–6) (1998) 69.
[24] A. Saada, B. Siffert, E. Papirer, J. Colloid Interface Sci. 174 (1) (1995) 185.
[25] G. González, M.B.C. Moreira, Colloids Surf. 58 (3) (1991) 293.
[26] H. Gaboriau, A. Saada, Chemosphere 44 (7) (2001) 1633.
[27] M. Szymula, A.W. Marczewski, Appl. Surf. Sci. 196 (1–4) (2002) 301.
[28] T. Pernyeszi, Á. Patzkó, O. Berkesi, I. Dékány, Colloids Surf., A 137 (1–3) (1998) 373.
[29] S. Acevedo, M.A. Ranaudo, C. García, J. Castillo, A. Fernández, M. Caetano, S. Goncalvez, Colloids Surf., A 166 (1–3) (2000) 145.
[30] H. Groenzin, O.C. Mullins, Energy Fuels 14 (3) (2000) 677.
[31] M. Castro, J.L.M. de la Cruz, E. Buenrostro-Gonzalez, S. López-Ramírez, A. Gil-Villegas, Fluid Phase Equilib. 286 (2) (2009) 113.
[32] A. Hassan, S. Ahmed, M.A. Ali, H. Hamid, T. Inui, Appl. Catal., A 220 (1–2) (2001) 59.
[33] N.N. Nassar, Energy Fuels 24 (8) (2010) 4116.
[34] O.P. Strausz, T.W. Mojelsky, E.M. Lown, Fuel 71 (12) (1992) 1355.
[35] D.C. Montgomery, G.C. Runger, Applied Statistics and Probability for Engineers, fourth ed., John Wiley & Sons, New York, 2006.
[36] A.W. Coats, J.P. Redfern, Nature 201 (4914) (1964) 68.
[37] B.L. He, Q. Song, S. Xu, Q. Yao, Presented at the 5th Asia-Pacific Conference on Combustion, The University of Adelaide, Adelaide, Australia, 2005 (unpublished).
[38] J. Li, R. Yan, B. Xiao, D.T. Liang, L. Du, Environ. Sci. Technol. 42 (16) (2008) 6224.
[39] K. Yanagisawa, T. Suzuki, Fuel 72 (1) (1993) 25.